Self-Organization of InAs/InP Quantum Dot Multilayers: Pseudophase Diagram Describing the Transition from Aligned to Antialigned Structures

A. Lévesque,[1] N. Shtinkov,[2] R. A. Masut,[1] and P. Desjardins[1]

[1]*Regroupement québécois sur les matériaux de pointe (RQMP) and Département de génie physique, École Polytechnique de Montréal, P.O. Box 6079, Station Centre-Ville, Montréal, QC H3C 3A7 Canada*

[2]*Department of Physics, University of Ottawa, Ottawa, Ontario, Canada K1N 6N5*

(Received 28 February 2007; published 28 January 2008)

Based on experimental observations for the InAs/InP(001) system and atomistic strain calculations using Keating's valence force field method, we propose a pseudophase diagram describing the regimes of 3D self-organization in quantum dot (QD) multilayers. The combined experimental and theoretical analyses—varying the spacer thickness (H), QD height (h), base (b), and lateral spacing (D)—indicate that the vertically aligned to antialigned transition occurs for a critical value of H/D which increases weakly with b/D, while varying h has virtually no effect on the transition point.

DOI: 10.1103/PhysRevLett.100.046101 PACS numbers: 68.65.Hb, 81.05.Ea

Much effort has been devoted to achieve periodicity and size uniformity of self-assembled semiconductor quantum dot (QD) structures grown in the Stranski-Krastanov mode for device applications. Improving dot size uniformity is deemed essential to optimize QD-based device performance [1,2]. It was observed that the strain-driven 3D self-organization occurring when stacking multiple QD layers leads to an improved uniformity in QD size and distribution [3–6]. Two regimes of vertical organization have been reported: (i) vertical alignment (VA), when the QDs grow on top of those from the previous layers and (ii) antialignment (AA), when the QDs are positioned between QDs from the previous layer. While the aligned regime is characterized by larger nanostructures from one layer to the next [3,5,7–10], anticorrelated structures present much more uniform island sizes and shapes throughout the multilayer [7–10]. A detailed understanding of the physical origins of such phenomena is a prerequisite for obtaining the required three-dimensional arrangement for a particular application.

It was initially believed, based on strain-minimization arguments, that a preferential site for QD nucleation is created on the surface directly above a buried QD because of the matrix deformation at this position [3,11]. While this treatment provides a simple, intuitive explanation for the aligned growth of successive QD layers, it cannot describe the antialigned regime observed in PbSe/PbTeEu [7], InGaAs/GaAs [8], and Ge/Si [9] QD multilayers, and in InAs/InP quantum stick stacks [10]. Two approaches were proposed to explain the appearance of this regime. (i) Calculations based on a single embedded quantum dot by Holy *et al.* [12] have shown that the minimum of the elastic energy on the surface above an isolated QD can be displaced from the vertical due to strain anisotropy. (ii) Based on energy-minimization calculations for a system composed of two planes of fully grown 2D islands, one embedded and one on the surface, Shchukin *et al.* [13] have demonstrated that the overlap of the strain fields of buried QDs can favor their antialignment. Case (i) tends to ignore the overlap of strain fields, while it is not obvious that case (ii) appropriately represents epitaxial growth in the kinetic regime: islands nucleate and grow on the strained surface; they do not move on the surface once grown. Recent experimental results have shown that while strain anisotropy is a determining parameter in samples with low island densities, the overlap of strain fields of neighboring islands leads to antialignment of QDs in higher density structures [14]. Furthermore, the transition between regimes depends on island plane separation distance, QD size, and areal density in a complex manner that still needs to be clarified [14].

Unfortunately, the only parameter that can easily be varied experimentally is the spacer thickness, although the growth conditions can be tailored to modify the QD geometry and areal density to a certain extent [15]. Experimental studies have demonstrated that increasing the spacer thickness H leads to a transition from aligned to antialigned nanostructures [7–10], and then to a random growth regime [7,11]; theoretically, this has been confirmed using continuous strain calculations [7,16] and kinetic Monte Carlo (KMC) simulations [17].

The effect and importance of other parameters (dot base, height, and lateral spacing), however, have not been systematically investigated either experimentally or theoretically. KMC simulations [17] have shown a transition from AA to uncorrelated growth and then to VA with increasing coverage. Shchukin *et al.* [13] identified the lateral dot spacing as an important parameter determining the correlation behavior of successive layers for 2D islands (no shape effect). The effect of dot size was the subject of a few theoretical studies: one found a transition from VA to AA with the increase of H/h without actually changing the dot height h [16], and another with the increase of the ratio between H and the dot base size b, varying b but keeping

the shape (aspect ratio) constant [7]. Although they reproduce certain experimental results for different systems (PbSe/PbEuTe, CdSe/ZnSe, InAs/GaAs), these studies have limited predictive value because they do not account for all structural parameters.

In this Letter, we present the results of an investigation of the three-dimensional self-organization of self-assembled InAs/InP(001) QD stacks. The combined experimental and theoretical analysis—varying all multilayer parameters [spacer thickness (H), QD dimensions (height (h), and base (b)) and lateral spacing (D)]—indicate that the vertically aligned to antialigned transition occurs for a critical value of H/D which varies weakly with b/D and that the value of h has no incidence on the transition point. We present a simple pseudophase diagram describing the type of vertical ordering as a function of these two parameters for InAs/InP(001) QDs, which is corroborated by experimental results.

The multilayers, comprising from 5 to 20 periods, were grown by low-pressure metalorganic vapor phase epitaxy in a cold-wall reactor described in [18]. We used trimethylindium (TMIn), tertiarybutylarsine (TBAs), and tertiarybutylphosphine (TBP) as precursors and Pd-purified hydrogen as the carrier gas. Quantum dot multilayers were deposited with a susceptor temperature T_s of 500 °C on an InP(001) oriented substrate, sandwiched between a buffer (120 nm) and a capping InP layer (100 nm), both grown at $T_s = 600$ °C. For each QD layer, the deposition of 3–7 ML of InAs was followed by a 60 s growth interruption under a $TBAs/H_2$ ambient to promote island formation [15]. The gas interruption sequence required to obtain abrupt interfaces has been described in [15]. The resulting islands have a nominal aspect ratio (height-to-base ratio) of 0.15–0.25. Their size and areal density were varied by changing two growth parameters: the growth rate (with TBAs flux constant) and the quantity of InAs deposited. Cross-sectional scanning transmission electron microscopy (STEM) observations were carried out at 200 kV on JEOL 2010F and 2100F instruments. A high-angle annular dark-field detector (HAADFD) was used in order to obtain Z (chemical) contrast.

Figure 1 presents typical STEM images of (a) a sample that presents aligned islands ($H = 21$ nm) and (b) an antialigned nanostructure stack ($H = 38$ nm). While Fig. 1(a) presents pure Z contrast that reveals the real island shape, we left a diffraction contribution in Fig. 1(b) in order to easily locate the quantum dots. The inset in Fig. 1(a) presents a typical truncated pyramidal island with 25° side angles that can be attributed to (113) facets. It should be noted that, in Fig. 1(b), the density and size of islands for the fifth layer are very low due to a change in the growth conditions for the last layer on this particular sample [19].

By varying the multilayer parameters, we have shown that organizational behavior depends not only on spacer layer thickness H (varied between 11 and 99 nm), but also

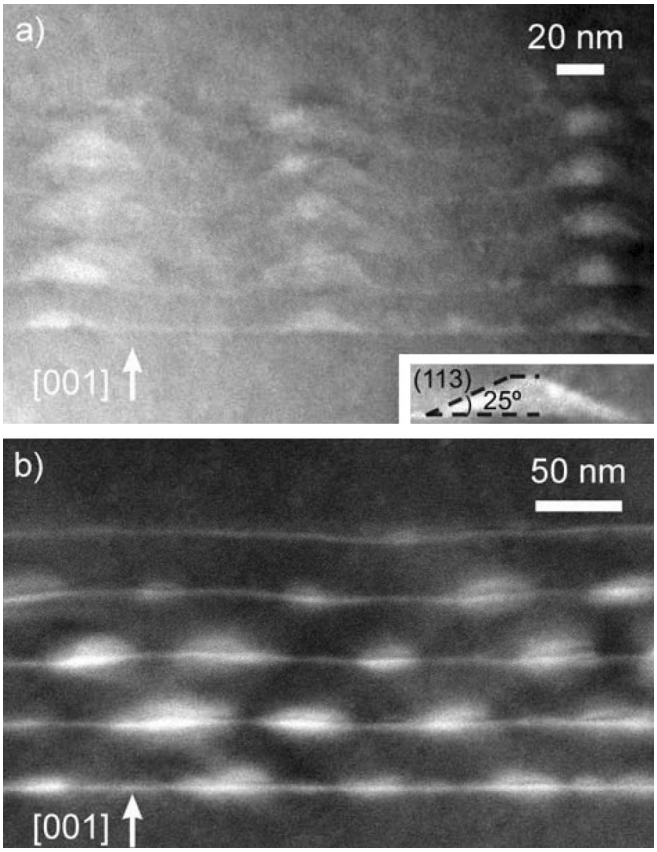

FIG. 1. HAADFD STEM images ([110] zone axis) of two samples showing (a) vertical alignment ($H = 21$ nm) and (b) antialignment of islands ($H = 38$ nm). The inset in (a) presents a typical truncated pyramidal island.

on the dot separation distance and/or size (height: $5 \leq h \leq 18$ nm; base: $25 \leq b \leq 85$ nm) of the first layer deposited (fully coherent islands). The results are summarized in Fig. 2 (the pertinence of this choice of axis will become obvious later). Experimental measures were obtained from cross-sectional STEM, so the values of D correspond really to projections on {110} planes. As can be seen in Fig. 2, in these samples the 3D self-organization regimes—VA (solid circles), AA (squares), uncorrelated (triangles)—appear sequentially with increasing H/D values. Indeed, vertical alignment is favored for low density (large D) samples of the order of 10^9 cm^{-2} with relatively large H (up to 68 nm), while for a multilayer with a smaller D of around 90 nm ($\sim 10^{10}$ cm^{-2}), an antialigned stacking of the QDs is observed for 38 nm-thick spacer layers. None of the other parameters among the ones suggested in the literature allow a separation of the stacking types of our samples. Our experimental data, however, do not permit to unambiguously isolate the effect of the island size (neither h nor b) on the organization regime from that of the separation distance D since these parameters are highly correlated for self-assembled QDs (increasing island size generally comes with a decrease of areal density [15]).

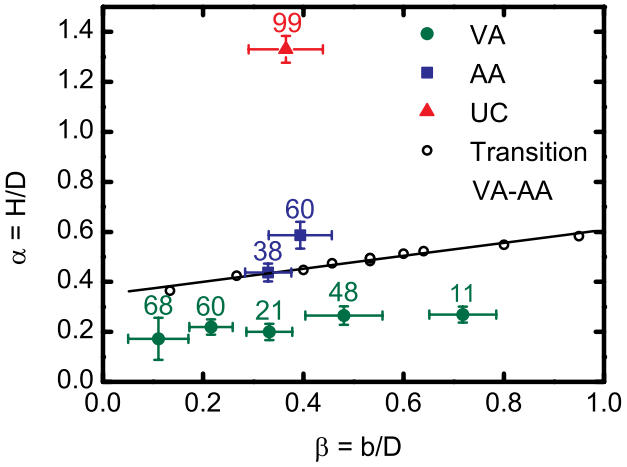

FIG. 2 (color online). Pseudophase diagram showing experimental results for VA, AA, and uncorrelated (UC) stacking, with spacer thickness values (in nm). The error bars correspond to the standard deviations. Calculated critical points (○) are presented with linear fit for the VA-AA transition.

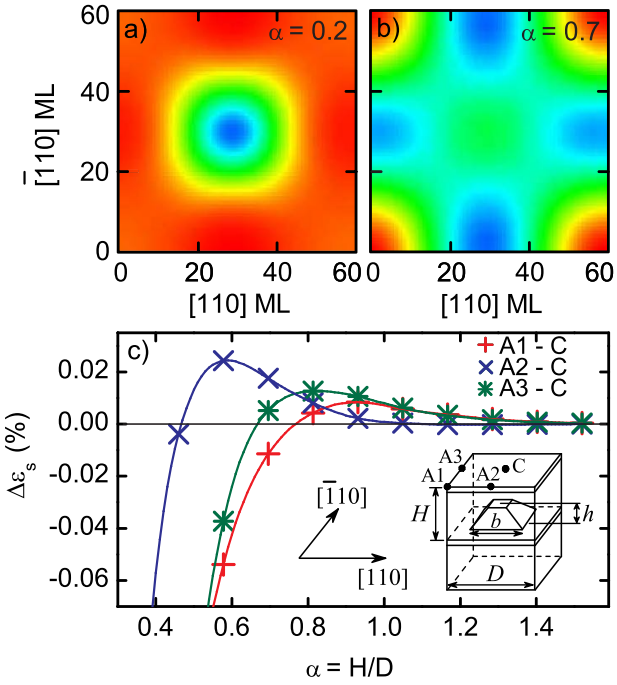

FIG. 3 (color online). Hydrostatic strain distribution (normalized, blue is minimum) for $D = 60$ ML (24.9 nm), $b = 32$ ML (13.3 nm), $h = 8$ ML (2.4 nm), and spacers H of (a) 19 ML (5.6 nm) and (b) 59 ML (17.3 nm). (c) Differences in the surface misfit strain $\Delta\varepsilon_s$ between an antialigned ($A1$–$A3$) and the aligned (C) position on the surface vs $\alpha = H/D$ near the transition VA-AA. The inset shows the geometry of the structures used in the simulations and the positions of points $A1$–$A3$ and C on the surface.

In order to systematically investigate the effect of h and b, we have carried out atomistic strain calculations using Keating's valence force field method [20] with the parameters of Martins and Zunger [21]. The model structure [see the inset of Fig. 3(c)] consists of an InP(001) substrate, an array of InAs QDs lying on a wetting layer (WL), an InP spacer layer, and a second InAs WL with a free unreconstructed surface. The WLs are As terminated, with topmost atoms bonded along the [110] direction. The atomic coordinates are relaxed using a conjugate-gradient algorithm until a minimum of the elastic energy is found. To simulate strained growth on InP substrate, the in-plane lattice constant is kept equal to that of InP and only the positions of the atoms in the bottom layer of the substrate are fixed. This is essential for obtaining a realistic strain field since it allows the structure to relax below the QD. We have fixed the substrate thickness at 18 nm since increasing it above this value does not further modify the resulting strain profiles. The QDs are shaped as truncated square pyramids with (113) side facets as observed by TEM, and the array is laterally periodic along the [110] and [$\bar{1}$10] axes. We have calculated 11 different structure geometries, varying independently each of the parameters of the buried QD layer: lateral period $16.6 \leq D \leq 29$ nm; QD base $3.3 \leq b \leq 15.8$ nm; QD height $1.2 \leq h \leq 3.6$ nm. The simulated WLs are one monolayer (0.3 nm) thick, and the thickness of the spacer layer H (including one WL—see Fig. 3) was varied between 5.6 and 38 nm. The entire structures consist of between 5×10^5 and 2×10^6 atoms. We verified the scaling by doubling the size of every parameter in an entire structure and confirmed that it had no incidence on the results.

For each QD layer geometry, we have calculated the evolution with spacer layer thickness H of the hydrostatic strain [typical results are shown in Figs. 3(a) and 3(b)] and the corresponding surface misfit strain ε_s [22]. Nucleation of a QD is most probable at the positions on the surface corresponding to a minimum of ε_s (smallest lattice mismatch with InAs, which is equivalent to the minimum of the surface elastic energy invoked in Refs. [6,12]). This minimum occurs either in the central position C (above the buried dot) or in one of the three symmetry points $A1$, $A2$, or $A3$ situated between the QDs (note that $A3$ is undistinguishable from $A1$ and $A2$ by STEM observations). The strain in each of these four points depends on H in a complex way. However, the detailed analysis of the calculation results shows that the differences between ε_s at these points have remarkably similar dependences on the dimensionless parameter $\alpha = H/D$. Typical dependences of $\Delta\varepsilon_s = \varepsilon_s(A) - \varepsilon_s(C)$ on α are presented in Fig. 3(c) for the three positions $A1$–$A3$. Note that since InAs is compressively strained ($\varepsilon_s < 0$), a negative difference $\Delta\varepsilon_s$ means that the top InAs WL is less strained at the central point C. From Fig. 3(c), one can follow the evolution of the alignment regime with increasing spacer thickness. For thin spacers the aligned growth is favored (all $\Delta\varepsilon_s$ are negative). With increasing H, there is a transition to antialigned growth as the strain energy minimum shifts to $A2$

($\alpha > 0.47$) and later to $A3$ ($\alpha > 0.78$). This difference between those two directions originates from the bond direction (C-$A3$ axis) in the WL, which makes it harder for the layer to deform along [110] as compared with $[\bar{1}10]$ (C-$A2$ axis). For thick spacers, the strain at the surface becomes uniform and random (uncorrelated) growth can be expected.

We have further detailed our analysis by considering the effect of the different parameters on the critical ratio α^{cr} for the VA-AA transition. When independently varied, the dot height h has no significant effect on the critical spacer thickness H^{cr} for which the transition occurs, contrary to what was assumed by some authors [16]. However, our calculations indicate that increasing the dot base width b increases H^{cr}. The analysis of our calculations thus justifies the choice of variables α and β in Fig. 2. All simulations results (open circles) have been added to our experimental data to form a pseudophase diagram describing the transition between VA and AA regimes. One can see that there is an excellent agreement between our theoretical and experimental results. The calculated transition points can be fitted with a linear curve, so the critical H/D ratio can be expressed as $\alpha^{cr} = 0.26\beta + 0.35$, where $\beta = b/D$ is equal to the square root of the surface coverage. Therefore, the ratio $\alpha = H/D$ is the dominant parameter determining the self-organization type, and, as expected, the VA regime is always favored for small spacer thicknesses (positive y intercept). Preliminary calculations for other materials (Ge/Si and InAs/GaAs) indicate a weak effect of the elastic anisotropy of the materials: α^{cr} tends to be slightly lower for higher anisotropy materials (consistent with Pei's results [16]). This is supported by the fact that experimental data obtained from the literature for In(Ga)As/GaAs [8,14] and (Si)Ge/Si [9] systems also fit well our diagram of Fig. 2.

In conclusion, we have shown, using a combination of atomistic calculations and experimental observations, that the type of self-organization in epitaxial quantum dot multilayers is mainly governed by the spacer layer thickness and the areal density of islands, but there is also a less important effect of their lateral dimension. One should thus be able to determine with this pseudophase diagram the range of spacer thicknesses required to obtain the desired stacking type from the characteristics of a single layer deposited.

The authors acknowledge the technical assistance of Mr. Joël Bouchard and the contribution of Pr. G. Botton (McMaster University) for TEM measurements. This work was supported by the Natural Sciences and Engineering Research Council of Canada (NSERC) and the Canada Research Chair Program.

[1] L. V. Asryan and R. A. Suris, Semicond. Sci. Technol. **11**, 554 (1996).
[2] J. Phillips, J. Appl. Phys. **91**, 4590 (2002).
[3] J. Tersoff, C. Teichert, and M. G. Lagally, Phys. Rev. Lett. **76**, 1675 (1996).
[4] M. K. Zundel *et al.*, Appl. Phys. Lett. **71**, 2972 (1997).
[5] E. Mateeva *et al.*, Appl. Phys. Lett. **71**, 3233 (1997).
[6] G. Springholz *et al.*, Science **282**, 734 (1998).
[7] G. Springholz *et al.*, Phys. Rev. Lett. **84**, 4669 (2000).
[8] X.-D. Wang *et al.*, Appl. Phys. Lett. **85**, 1356 (2004).
[9] O. Kermarrec, Y. Campidelli, and D. Bensahel, J. Appl. Phys. **96**, 6175 (2004).
[10] N. Chauvin *et al.*, J. Cryst. Growth **275**, e2327 (2005).
[11] Qianghua Xie *et al.*, Phys. Rev. Lett. **75**, 2542 (1995).
[12] V. Holy *et al.*, Phys. Rev. Lett. **83**, 356 (1999).
[13] V. A. Shchukin *et al.*, Phys. Rev. B **57**, 12 262 (1998).
[14] M. Gutiérrez *et al.*, Appl. Phys. Lett. **88**, 193118 (2006).
[15] H. Marchand *et al.*, J. Electron. Mater. **26**, 1205 (1997).
[16] Q. X. Pei, C. Lu, and Y. Y. Wang, J. Appl. Phys. **93**, 1487 (2003).
[17] M. Meixner and E. Scholl, Phys. Rev. B **67**, 121202 (2003).
[18] P. Cova *et al.*, Can. J. Phys. **69**, 412 (1991).
[19] For this sample, a full InP spacer layer was not deposited on the last layer at 500 °C before interrupting the growth and increasing T_s to 600 °C, but only a precapping layer of about 5 nm. This does not affect the conclusions of this work, since the antialignment behavior in this sample is clearly observed in the three preceding QD layers (see Fig. 1). The experimental data (QD dimensions and lateral spacing), used in the phase diagram in Fig. 2, are obtained from the first QD layer of each sample.
[20] P. N. Keating, Phys. Rev. **145**, 637 (1966).
[21] J. L. Martins and A. Zunger, Phys. Rev. B **30**, 6217 (1984).
[22] The surface misfit strain ε_s with respect to InAs is calculated along the direction of the bonds between the In adatoms and the sample surface: $\varepsilon_s = (l - l_0)/l$, where l is the $[\bar{1}10]$ distance between two As atoms on the surface and l_0 is the corresponding distance in unstrained InAs.